Ferrimagnetic resonance and magnetoelastic excitations in magnetoelectric hexaferrites

Carmine Vittoria

Phys. Rev. B **92**, 064407 — Published 4 August 2015

DOI: 10.1103/PhysRevB.92.064407

Ferrimagnetic Resonance and Magneto-elastic Excitations in Magneto-Electric Hexaferrites

Carmine Vittoria, Northeastern University, Boston, MA 02115

Abstract

Static field properties of magneto-electric hexaferrites have been explored extensively in the past five years. In this paper dynamic properties of magneto-electric hexaferrites are being explored. In particular, effects of the linear magneto-electric coupling (α) on ferrimagnetic resonance (FMR) and magneto-elastic excitations are being investigated. A magneto-elastic free energy which includes Landau-Lifshitz mathematical description of a spin spiral configuration is proposed to calculate FMR and magneto-elastic excitations in magneto-electric hexaferrites. It is predicted that the ordinary uniform precession FMR mode contains resonance frequency shifts that are proportional to magneto-electric static and dynamic fields. The calculated FMR fields are in agreement with experiments. Furthermore, it is predicted at low frequencies (~MHz ranges), near zero magnetic field FMR frequencies, there is an extra uniform precession FMR mode besides the ordinary FMR mode which can only be accounted by dynamic magneto-electric fields. Whereas the FMR frequency shifts in the ordinary FMR mode due to the α coupling scale as α, the shifts in the new discovered FMR mode scale as α^2.

Also, magneto-elastic dispersions were calculated and it is predicted that the effect of the α coupling are the following: 1. The strength of admixture of modes and splitting in energy between spin waves and transverse acoustic waves is proportional to α. 2. The degeneracy of the two transverse acoustic wave modes is lifted even for relatively low values of α. Interestingly, at low frequencies near zero field FMR frequencies the surface spin wave mode branch flip-flops with the volume spin wave branch whereby one branch assumes real values of the propagation constant and the other purely imaginary upon the application of a static electric field.

I Introduction

Magneto-Electricity has been discovered in single phase bulk [1-10] and thin film [11] of hexaferrites. The linear magneto-electric (ME) coupling parameters, α, of hexaferrites at room temperature are fairly high [1-11] in comparison to other types of single phase materials [12-17] and laminated composite structures [18]. Potential for new applications in medical sensors, recording media, computer and electronic integrated circuits (IC) and wireless communication networks appear to be promising. In a ME material the application of a magnetic field, **H**, induces an electric polarization, **P**, and this is referred to as a direct ME effect [19]. In the converse [19] ME effect the application of an electric field, **E**, induces magnetic polarization or **M**. Landau-Lifshitz [20] proposed in 1957 the possibility of linear relationship between the electric field, **E**, and magnetic field, **H**. Dzyaloshinski [21] showed that such linear relationship between **E** and **H** may be possible, if spins at different sites were non co-linear. The notion of non-collinearity of the spins was re-enforced theoretically by Moriya [22] in considering mechanisms of the local magnetic anisotropy and exchange coupling between spin sites extending single ion models [23]

for magnetic anisotropy. Experimental confirmation of magneto-electricity was discovered in Cr_2O_3 by Astrov [24] and Folen and Rado [25].

Since the discovery of magneto-electricity various theoretical models [26-31] have been proposed to explain magneto-electricity in terms of spin non-collinearity and specifically with spin spiral configurations. Most of these models apply to single phase ME materials and not pertaining necessarily to hexaferrites. A thermodynamic argument was proposed [32] to model magneto-electricity in hexaferrites. The model may simply be summarized briefly as follows. The ME coupling parameter, α, in hexaferrites is anisotropic and it scales as the product of the magnetostiction constant and piezoelectric strain coefficient. The thermodynamic argument is of sufficient generality that it may be applicable to materials other than hexaferrites. In this paper we consider dynamic field excitations in ME hexaferrites and utilize the M-type hexaferrite magnetic structure as a model for our calculations. This is the simplest magnetic and crystal structure [33] to analyze and still exhibiting ME effects [10]. The arguments to be presented here apply equally well to other hexaferrites [35-36] and in fact our theoretical results are also applicable to Z-type hexaferrites.

The spin spiral configuration in this system is due to a number of factors. M-type hexaferrites consist of four spinel "blocks" (RSR*S*), where the S block contains octahedral (2a) and tetrahedral (4f) sites and R block octahedral (2a) and nearly octahedral (bypyramidal-2b). The * implies 180 degrees rotation relative to the unmarked block [35]. Strong exchange coupling aligns spins anti-parallel to each other in each block forming a ferrimagnetic magnetic structure. However, Sr substitutes in the usual barium sites located in the R or R* block near one of the octahedral sites [35] distorting or straining the chemical bonds near that site. The effects of Sr substitutions on local strains and spin coupling between sites are described in Ref [10]. Since Co and Ti ions only substitute into octahedral sites located in the R or R* block and in the periphery (12k sites) of the R blocks, there are two ramifications: 1) The local magnetic anisotropy in the R block is much stronger than usual, but, more importantly, it assumes a uniaxial axis at oblique angle to the c-axis. 2) The exchange coupling between R and R* blocks is weakened, since Ti ions are not magnetic and are located at the 12k sites. It is the weakening of the exchange coupling that allows for the local anisotropy a preferential alignment of the local spins and still maintaining the out of phase spin alignment from block to block. We believe that this is the recipe for a spin spiral configurations and the phenomena of magnetoelectricity in M-type hexaferrites. This physical picture may be applicable to other types of hexaferrites as well (Y and Z-type). As stated above we are interested in the dynamic field excitations, magnetic or elastic, in ME hexferrites. Dynamic field excitations include ferromagnetic resonance, magnetic susceptibilities and wave propagation in a magneto-elastic medium as in a ME hexaferrite.

II Free Energy Representation of Spin Spiral Configuration

The quantum representation of the spin spiral by Dzyaloshinski [21] and Moriya [22] included the following interaction form

$$D \bullet (S_i \times S_j) \ , \qquad (1)$$

where $\vec{D}$ is a vector proportional to exchange and local spin orbit and crystal fields interaction parameters at local sites i and j. In order for this interaction term to contribute to potential energy, spins at different sites could not be parallel to each other as in a spin spiral configuration, for example. Landau-Lifshitz [20] introduced a semi-classical description of the above quantum form as follows (CGS)

$$F_{LL}(ergs/cm^3) = -\frac{K_{LL}}{M^2} M \bullet (\nabla \times M), \qquad (2)$$

where F_{LL} is the free energy of a spin spiral configuration as derived by Landau-Lifshitz [20], K_{LL} is a anisotropy energy parameter in units of ergs/cm^2 and is proportional to the parameter D in eq. 1. M is the magnetization vector representing the spin variables over a relative large volume compared to a unit cell. Clearly, eq. 1 is microscopically applicable to single spins, whereas eq. 2 applies to macroscopic levels of interaction. Assuming that the transition from microscopic to macroscopic representations may be acceptable, we explore the predictions of eq. 2. For simplicity, $\vec{M}$ may be expressed as follows

$$M = M_{\|} a_z + M_{\perp}(a_x \cos \beta z - a_y \sin \beta z), \qquad (3)$$

where a_x ,a_y and a_z are unit vectors in the x, y and z directions, M|| is the component of the magnetization along the c-axis or the z-axis, see Fig. 1, $M_{\perp}$ is the component perpendicular to the c-axis, $\beta = 2\pi/\lambda$, and λ is the wavelength of the helical or spin spiral configuration along the c-axis.

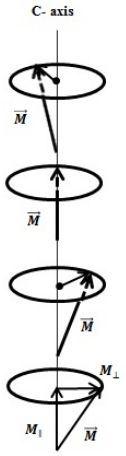

Fig. 1 Spin Spiral configuration along C-axis for M-type ME hexaferrites and perpendicular to C-axis for Z-type ME hexaferrites.

In order for this description to be valid λ >> c, where c is the lattice constant along the c-axis (~23A). Substituting eq. 3 into eq. 2 yields

$$F_{LL} = -K_{LL}\beta(\frac{M_{\perp}}{M})^2 \equiv -K(\frac{M_{\perp}}{M})^2. \qquad (4)$$

This is recognized as a classical uniaxial magnetic anisotropy energy term with a uniaxial axis along the c-axis [37]. This is interesting in that the macroscopic Landau-Lifshitz representation basically averages all local uniaxial anisotropy energies into one single expression (eq. 4), although the local uniaxial axis is at an oblique angle with respect to the c-axis, see Fig. 1. This is not surprising in view of the fact that the sum of uniaxial anisotropy energies still results into one single uniaxial energy term as above. We will adopt the Landau-Lifshitz macroscopic representation and designate the uniaxial anisotropy energy parameter as K_{ss} or K_{θ}. Clearly , K_{ss} is related to the parameters K_{LL}, K and D (eqs. 1-4). The corresponding uniaxial magnetic anisotropy magnetic field, H_{ss} , is defined as $2K_{ss}/M$ and it applies to a spin spiral configuration in a ME hexaferrite ($\alpha \neq 0$). For the case $\alpha=0$ in normal hexaferrites it is meaningful to define also a uniaxial anisotropy field, H_{θ}, equal to $2K_{\theta}/M$. Thus, K_{ss} plays a dual role depending on the value of α, 0 or $\neq 0$.

III Free Energy of ME Hexaferrite

The total free energy, F(ergs/cm^3), is comprised of magnetic, F_M, and electric, F_E, free energies or

$$F = F_M + F_E , \qquad (5)$$

where

$$F_M = -HM_z + 2\pi M_z^2 - K_{ss}\left(\frac{M_z}{M}\right)^2 - \left(\frac{A}{M^2}\right)M \bullet \nabla^2 M$$
$$- K_{\varphi}[M_x^6 - M_y^6 + 15M_x^2 M_y^2 (M_y^2 - M_x^2)] - \alpha M \bullet P \qquad (6)$$

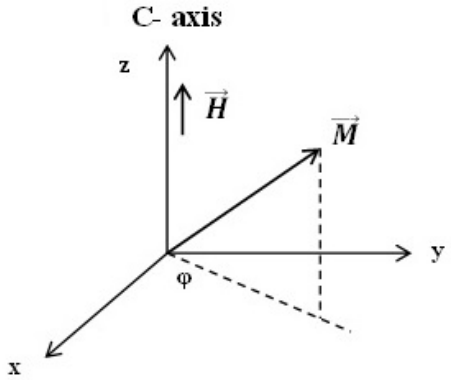

Fig. 2. Magnetic field orientations relative to the C-axis.

The external magnetic field, H, is applied normal to the film plane and parallel to the c-axis, see Fig. 2. The second term in F_M is the demagnetizing energy and the third term the macroscopic uniaxial anisotropy energy as described in section II. The energy parameter K_{ss} is analogous to the parameter K_ϑ usually designated in typical hexaferrites [35]. The subscript "ss" is to remind the reader that this parameter corresponds to a spin spiral configuration. The fourth term is the ordinary semi-classical exchange coupling term and is often referred to as the exchange stiffness constant and the fifth term is the magnetic anisotropy energy corresponding to magnetization directions in the azimuth plane (normal to the c-axis). Typically, the magnetic anisotropy field associated with this energy term is in the order of 20-50 Oe [38]. Finally, the last term is the magneto-electric coupling energy term. The coupling parameter α is treated as a scalar. In general it is anisotropic and may be represented as a tensor [32]. For now it suffices for the purpose of demonstrating the formalism of the calculations. The polarization vector is a complicated function of the internal strain, as it must be for a ME medium like the hexaferrites. In a ME medium the strain coefficient tensor [d] couples [P] to the stress tensor [T] or

$$[P] = [d][T], \tag{7}$$

where [d] for hexagonal crystal structure is of the form [39]

$$[d] = \begin{bmatrix} 0 & 0 & 0 & 0 & d_5 & 0 \\ 0 & 0 & 0 & d_4 & 0 & 0 \\ d_1 & d_1 & d_3 & 0 & 0 & 0 \end{bmatrix}. \tag{8}$$

The stress tensor [T] for hexagonal structure is also cited in Ref. [39] and utilizing eq. (7) yields the polarization components as follows

$$P_x = d_5 C_{44} \in_{zx} \quad ; \quad P_y = d_5 C_{44} \in_{zy} \quad ; \quad P_z \approx d_3 C_{33} \in_{zz} + \varepsilon_0 \chi_e V / t \,.$$

The strain fields are $\in_{zx}, \in_{zy}$ and $\in_{zz}$, V is the DC voltage applied across a film or a slab, and t is the thickness of the film or slab. Usually, the magneto-electric coupling is expressed as $-\alpha' \vec{E} \bullet \vec{H}$. The connection between the two alphas is simply $\alpha' = \chi_m \alpha \chi_e$, where χ_m and χ_e are the magnetic and electric susceptibilities, respectively. The free energy for the electric system including strain fields is shown below [32]

$$\begin{aligned} F_E = & -P \bullet E + \frac{1}{2}\left[C_{33} \in_{zz}^{\ 2} + C_{11}(\in_{xx}^{\ 2} + \in_{yy}^{\ 2}) + C_{44}(\in_{zx}^{\ 2} + \in_{zy}^{\ 2})\right] \\ & + C_{12} \in_{xx} \in_{yy} + C_{13} \in_{zz} (\in_{xx} + \in_{yy}) + \frac{1}{4}(C_{11} - C_{12}) \in_{xy}^{\ 2} \end{aligned} \tag{9}$$

The first term is the polarizing electric energy and the remaining terms are elastic energy terms for a hexagonal crystal structure. The C's are the elastic stiffness modulus constants and $\in_{ij}$ are the strain fields defined in terms of elastic displacements U_i as

$$\in_{ii}=\frac{\partial U_i}{\partial x_i} \quad ; \quad \in_{ij}=\frac{\partial U_i}{\partial x_j}+\frac{\partial U_j}{\partial x_i} \quad .$$

The subscripts indicate directions x,y and z. According to Ref. [32] the ME coupling α can be expressed in terms of the product of magnetostriction constants and piezoelectric strain coefficients. This implies that there is an alternative way to express the free energy that couples the magnetic system to the electric system. Either the coupling between the two systems is via α as in eqs. (6) and (9) or omit α in eq. (6) and introduce magnetostriction and piezoelectric strain parameters in eqs. (6) and (9). Let's now consider the alternative expression for the free energies. Extending Landau-Lifshitz [20] formalism to hexagonal crystal structures the magneto-elastic coupling

$$\begin{aligned} F_{mag-el} &= (a_1\alpha_1^{\,2}+a_3\alpha_3^{\,2})\in_{xx}+(a_1\alpha_2^{\,2}+a_3\alpha_3^{\,2})\in_{yy}+[a_2\alpha_3^{\,2}+a_3(\alpha_1^{\,2}+\alpha_2^{\,2})]\in_{zz} \\ &+a_4\alpha_1\alpha_2\in_{xy}+a_5\alpha_1\alpha_3\in_{xz}+a_5\alpha_2\alpha_3\in_{yz} \end{aligned} \qquad (10)$$

The a_i coefficients may be related to the magnetostriction constants [40]. For example, the coefficients a_i may be expressed in terms of the B_1 and B_2 magnetostriction coefficients for cubic symmetry crystals (see Ref. [41]). The key point of eq. (10) is that the strain is coupled to the magnetic system, where α_i are the directional cosines of $\vec{M}$ relative to the x,y and z coordinate system. The other half of the alternative methodology is to introduce the piezoelectric coupling in eq. (9) which couples the electric field or system to the strain. Basically, the mediator that couples the magnetic system to the electric system is the strain field. Thus, for example, the excitation of an electric field is coupled via the piezoelectric strain coefficient to the strain field. The strain field in turn is coupled to the magnetic system via the magnetostriction coupling as in eq. (10). For hexagonal crystal symmetry the piezoelectric coupling energy term takes on the following form

$$\begin{aligned} F_{piezo-el} &= -d_5C_{44}(\in_{zx}E_x+\in_{zy}E_y)-d_1[(C_{11}+C_{12})(\in_{xx}+\in_{yy})+2C_{13}\in_{zz}]E_z \\ &-d_3[C_{13}(\in_{xx}+\in_{yy})+C_{33}\in_{zz}]E_z \end{aligned} \qquad (11)$$

Thus, the addition of eqs. (10) and (11) to the free energy F would replace the coupling energy term containing α . Clearly, more parameters are introduced, but it is needed to explain, for example, anisotropic coupling between the two systems. However, anisotropic coupling could also be analyzed using a tensor α rather than a scalar α. We will not dwell on the merit of the two methodologies, but simply choose eq. (6) as a starting point. The object is to introduce the

formalism to calculate dynamic excitations in ME hexaferrites. Our formalism would also apply for either methodologies (eqs. (10) and (11) versus the inclusion of α coupling explicitly) as well. So far, we have assumed that ME hexaferrites exhibit piezoelectricity only. One should be aware that some ME hexaferrites may also be characterized as being ferroelectric. In that case terms like second, fourth order and higher even powers [42] of P may be added to the free energy. Furthermore, in polycrystalline ME hexaferrite of the Z-type [19] the material behaved electrostrictive implying that the relationship between strain and electric field was quadratic [42]. In such cases eqs. 10-11 would have to be modified in order to allow for the quadratic dependence on strain. The static fields equilibrium conditions and ferromagnetic resonance (FMR) may be calculated directly from the free energy [32] as follows.

1. Static Fields Equilibrium Conditions

In Fig. (2) directions of the various fields relative to the film surface and c-axis are shown. The equilibrium position of static M may be determined for H fields below and above magnetic saturation. At non-saturation the internal static field, H_0, is zero, but at saturation $H_0 \neq 0$. The total internal magnetic field, $H_i = H_0 + h_i$, may be determined by taking the magnetic gradient of F, where h_i is the internal dynamic magnetic field [37]. Thus,

$$H_i = H_0 + h_i = -\nabla_M F = (H - 4\pi M_Z + \frac{H_{ss}}{M} M_z)a_z + \alpha P, \quad (12)$$

where

$$H_{ss} = \frac{2K_{ss}}{M}, \ \mathrm{M_z} = \mathrm{M_{0z}} + \mathrm{m_z}, \ M_{0z} = M\cos(\theta), \ P = P_z a_z + p, \text{ and } P_z = \varepsilon_0 \chi_e V / t.$$

Upper case variables are static fields which are not time dependent and lower case variables are dynamic fields which are time dependent and they will be utilized later when FMR is discussed. Equating $\vec{H}_0$ to static fields yields the equation that

$$H_0 = (H - 4\pi M\cos\theta + H_{ss}\cos\theta + \alpha\varepsilon_0\chi_e V / t)a_z. \quad (13)$$

The internal static field is that field that aligns the internal magnetization, $\vec{M}_0$, along or parallel to $\vec{H}_0$, and, therefore, $H_0 \geq 0$. It is unphysical concept for H_0 to be less than zero. Setting $H_0 = 0$ yields the equilibrium static condition for non-magnetic saturation as

$$\cos\theta = \frac{H}{4\pi M - H_{ss}}. \quad (14)$$

Above equilibrium condition may be derived also from Smit-Beljers [43] methodology requiring $\frac{\partial F}{\partial \theta} = 0,$ whereby F is expressed in terms of θ and ϕ. In our representation, F is expressed explicitly in terms of static and dynamic fields. Typically, P_z is relatively small compared to H_{ss} and it has been omitted in above equilibrium condition. The magnetization component along H is

simply $M_H = M\cos\theta$ assuming single domain rotation, for example. Eq. (14) applies for $4\pi M \geq H_{ss}$ and the ME films being single crystal. For polycrystalline films the magnetic anisotropy field would average to zero and H_{ss} may be omitted in eq. (14). For $H_{ss} \geq 4\pi M$, the spontaneous magnetization alignment would be in the positive or negative z-directions as in M-type hexaferrites, but not in Z-type. Perhaps, magnetic multi-domain analysis may be more appropriate [44] for M-type hexaferrites. In summary, at magnetic saturation $H_0 = H - 4\pi M + H_{ss}$.

Similarly, H_0 may be derived for H in the film plane and it is equal to H, as in the case of Z-type hexaferrites, see Refs. [35] for description of different types of hexaferrites. In Fig. 3 M_H is plotted as a function of H for H parallel and perpendicular to the slab plane of a Z-type hexaferrite [45]. Clearly, the hard axis of magnetization was pointed along the c-axis or perpendicular to the slab plane, and the magnetic anisotropy energy is characterized as being planar. The deduced parameters from this data were the following: $4\pi M = 3100G$ and $H_\theta \approx 6500Oe$. Typically, for Y and Z-type hexaferrites $H_\theta >$ 9000 Oe [35]. The fact that technical magnetic saturation is not reached implies that it takes more field to align the canting of the spins at each site (see Fig. 3). Equivalently, H cannot overcome exchange fields between sites.

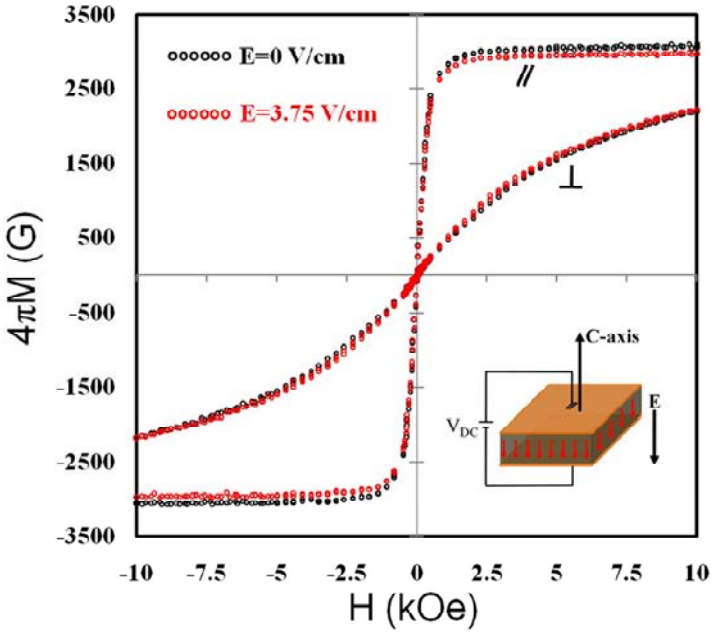

Fig. 3 Vibrating sample magnetometer (VSM) measurements of the magnetization versus magnetic field for H parallel (||) and perpendicular $(\perp)$ to the plane of the ME slab material (Z-type hexaferrite).

2. Ferrimagnetic Resonance Excitations in ME Hexaferrites

For H values below magnetic saturation H_0 = 0 and, hence, FMR may not be observed. In saturating fields FMR condition may be derived from the equation of motion of the dynamic components of the magnetization. The normal modes of FMR excitations are m_x and m_y for H applied normal to the film plane and m_x and m_z for H in the film plane (H along the y-axis). The equation of motion for M is then

$$\frac{1}{\gamma}\frac{dM}{dt} = M \times H_i \equiv M_0 \times h_i + m \times H_0 \quad \text{, where} \quad \gamma = g(2\pi \times 1.4 \times 10^6) rad/Oe \text{ , g} \sim 2. \qquad (15)$$

and

$$M = M_0 + m \quad ; \quad M_0 = Ma_z \quad ; \quad H_0 = (H - 4\pi M + H_{ss} + \alpha\varepsilon_0\chi_e V/t)a_z \quad ;$$

$$h_i = (-4\pi m_z + H_{ss}\frac{m_z}{M} + \alpha p_z)a_z + \alpha p \quad .$$

The equation of motion is linearized by omitting terms consisting of the product of two dynamic variables, p_z and m_z, since they are assumed to be small compared to linear terms in m_x or m_y and p_x or p_y. As such, the equation of motion simplifies to

$$j\frac{\omega}{\gamma}m_x = m_y H_0' \text{ , and}$$

$$j\frac{\omega}{\gamma}m_y = -m_x H_0' \quad , \quad \text{where } H_0' = H_0 - 4\pi\delta M \quad \text{and } \delta = \frac{\alpha p_x}{m_x} = \frac{\alpha p_y}{m_y} \quad .$$

Thus, the FMR condition becomes

$$\frac{\omega}{\gamma} = H_0' = H - 4\pi M + H_{ss} + \alpha\varepsilon_0\chi_e V/t - 4\pi\delta M \, . \qquad (16)$$

In the limit that α = 0 and no spin spiral configuration (K_{ss} =0) the FMR condition for H applied perpendicular to the film plane simplifies to the well-known result that [37]

$$\frac{\omega}{\gamma} = H - 4\pi M \, .$$

For $\alpha \neq 0$, the FMR condition is given in eq. (16). There are two observations to be made in this limit: 1) The FMR condition in eq. (16) contains a static field FMR resonance shift ($\alpha\varepsilon_0\chi_e V/t$) from the application of a DC voltage V. The dynamic field shift ($4\pi\delta M$) in eq. (16) is somewhat different from previous reports [1-10]. 2) For H = 0, eq. (16) predicts the so-called zero field FMR [41], if $H_{ss} > 4\pi M$ for single domain excitations. However, if magnetic multi-domains are formed for H = 0, zero field FMR is predicted for arbitrary values of H_{ss} . The zero field FMR resonance conditions are approximated as follows:

$$\frac{\omega}{\gamma} \approx H_{ss} - 4\pi M + \alpha\varepsilon_0\chi_e V/t - 4\pi\delta M \quad , \qquad (16a)$$

For single magnetic domain

$$\frac{\omega}{\gamma} \approx H_{ss} + \alpha\varepsilon_0\chi_e V/t - 4\pi\delta M \ , \qquad (16b)$$

For magnetic multi-domains [44].

In-plane FMR may be considered with the modification of the free energy. The Zeeman energy term or magnetizing energy term includes H along the y-axis, for example. Without going through the same formalism as above the FMR condition is quoted for in-plane FMR assuming Z-type hexaferrite as (we have data [45] for this hexaferrite). Since α≠0, we may write

$$(\frac{\omega}{\gamma})^2 = (H + 4\pi M + H_{ss} - 4\pi\delta M)(H - 4\pi\delta M) . \qquad (17)$$

In the limit that H = 0 eq. (17) implies that $(\frac{\omega}{\gamma})^2$ <0, assuming δ >0.

In the limit α= 0 eq. (17) reduces to the well-known result that [37]

$$(\frac{\omega}{\gamma})^2 = (H + 4\pi M + H_\theta)(H) .$$

It is pointed out that there is no static magnetic field shifts in the FMR condition as in eq. (16) upon application of DC voltage. This a direct result of the fact that α is assumed to be a scalar rather than a tensor. Let's now analyze recent [45] FMR resonance data, see Fig. 4, on Z-type hexaferrite utilizing the data [44] of Fig. 3. The deduced value of the g factor was g =1.90. The fact that g<2 implies that orbital contribution from Co substitutions contribute to the lowering of g value.

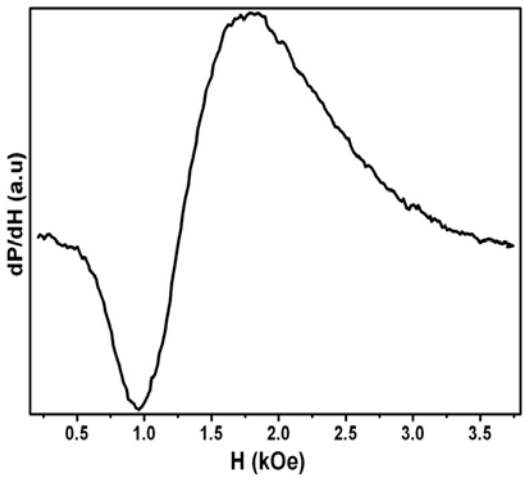

Fig.4 FMR of Z-type hexaferrite for H in the slab plane (see Fig. 3 also). dP/dH is the field derivative of the power absorbed by the sample in arbitrary units.

IV Magneto-elastic Excitations in ME Hexaferrites

The mediator that couples the magnetic system to the electric system is the strain fields in ME hexaferrites. Thus, elastic waves may be excited via the electric system, since the electric system is coupled to elastic waves by the piezoelectric strain coupling. The counterpart to piezoelectricity is the magnetostriction coupling in the magnetic system. The point of this exercise is to show that the ME α coupling takes into account all of these internal couplings "automatically". The proof of the latter statement is to substitute eqs. (10-11) into eqs. (6-9) and omit the α coupling term in eq. (6) and show that the same results are obtained either way. We will consider the simpler approach – scalar α coupling term only. The dispersion relation between frequency and propagation constant, k, is calculated for H perpendicular to the film plane whereby spin wave modes, elastic waves and electromagnetic propagation modes are excited. Although propagation of the waves is assumed to be perpendicular to the film plane or parallel to the c-axis, the formalism is applicable for arbitrary direction of k. The formalism involves the coupling of three sets of equations: magnetic equations of motion, elastic equations of motion and Maxwell's equations. The algebra encountered in coupling all three sets of equations is formidable, but electromagnetic effects due to Maxwell's equations can be included in ad-hoc manner [37] simplifying the formalism. Proof of the ad-hoc approach is given in the appendix.

The magnetic equations of motion can be readily extended to include elastic strain fields and spin wave fields using eqs. (15) as a starting point.

$$j\frac{\omega}{\gamma}m_x = m_y(H_0 + \frac{2A}{M^2}k^2) - M\alpha p_y\,, \tag{18}$$

$$j\frac{\omega}{\gamma}m_y = -m_x(H_0 + \frac{2A}{M^2}k^2) + M\alpha p_x\,, \tag{19}$$

where

$$p_x = d_5 C_{44} \in_{zx}\,, \text{ and}$$

$$p_y = d_5 C_{44} \in_{zy}\quad .$$

The Hamilton-Jacobi principle [46] is applied to obtain the elastic equations of motion and they are

$$\rho\frac{d^2U_x}{dt^2} = C_{44}\frac{\partial^2 U_x}{\partial z^2} - \alpha d_5 C_{44}\frac{\partial m_x}{\partial z}\ , \tag{20}$$

$$\rho \frac{d^2 U_y}{dt^2} = C_{44} \frac{\partial^2 U_y}{\partial z^2} - \alpha d_5 C_{44} \frac{\partial m_y}{\partial z}, \qquad (21)$$

$$\rho \frac{d^2 U_z}{dt^2} = C_{33} \frac{\partial^2 U_z}{\partial z^2}, \qquad (22)$$

where

ρ is the crystal density, A is the exchange stiffness constant [47] and U_i are elastic displacements. It can be shown that the same set of eqs. (18-22) can be derived by using eqs. (10-11). Assuming solutions of the form $e^{j(\omega t - kz)}$ and demanding non-trivial solutions of the field variables a dispersion relation is obtained by expanding the following determinant and setting it to zero.

$$\det \begin{bmatrix} -j\frac{\omega}{\gamma} & H_0 + \frac{2A}{M^2}k^2 & 0 & jk\alpha d_5 C_{44} & 0 \\ H_0 + \frac{2A}{M^2}k^2 & j\frac{\omega}{\gamma} & jk\alpha d_5 C_{44} & 0 & 0 \\ jk\alpha d_5 C_{44} & 0 & \omega^2 - \frac{C_{44}}{\rho}k^2 & 0 & 0 \\ 0 & jk\alpha d_5 C_{44} & 0 & \omega^2 - \frac{C_{44}}{\rho}k^2 & 0 \\ 0 & 0 & 0 & 0 & \omega^2 - \frac{C_{33}}{\rho}k^2 \end{bmatrix} = 0. \qquad (23)$$

Expanding the above determinant yields the following dispersion relation

$$(\omega^2 - \frac{C_{44}}{\rho}k^2)^2[(H_0 + \frac{2A}{M^2}k^2)^2 - \frac{\omega^2}{\gamma^2}] + 2(\omega^2 - \frac{C_{44}}{\rho}k^2)(H_0 + \frac{2A}{M^2}k^2)k^2 \frac{M}{\rho}\alpha d_5 C_{44} + k^4 \frac{M^2}{\rho^2}(\alpha d_5 C_{44})^4 = 0 \qquad (24)$$

The term $(\omega^2 - \frac{C_{33}}{\rho}k^2)$ multiplies the above eq. 24 so that it factors out and is equal to zero. Thus, the longitudinal acoustic mode is uncoupled to spin waves or the other two transverse acoustic branches or modes, and the dispersion relation is written as

$$\omega = k\sqrt{\frac{C_{33}}{\rho}} \equiv kv_L .$$

The longitudinal acoustic velocity is identified as $v_L = \sqrt{\frac{C_{33}}{\rho}}$. The two transverse branches or modes are degenerate for frequencies above and below the approximate FMR frequency or the crossing region between the spin wave branch and the two transverse acoustic modes, see Fig. 5. The transverse acoustic velocity is then $v_T = \sqrt{\frac{C_{44}}{\rho}}$. The following parameters were assumed for the plot of Fig. 5: $A = 0.4 \times 10^{-6} ergs/cm, \rho = 5.3, g = 2, 4\pi M = 1400G, d_5 = 1.1\text{x}10^{-11}$ m/v, C_{44} = $1.0\text{x}10^{12}$ ergs/cm^3, C_{33} =3C_{44}. The conversion of d_5 to CGS units is $3\text{x}10^4$. The uniform mode (k=0) FMR excitations occurs at H_0 =3500 Oe corresponding to a FMR frequency of 9.8 GHz. The spin wave branch (SW_1) intersects the two transverse acoustic branches, but only one is dynamically coupled to SW_1 branch, splitting the two branches at the intersection. The other spin wave branch SW_2 consists only of imaginary propagation constants, see Figs. 5-6. As such, this spin wave branch represents attenuating spin wave magnetization fields. It is often referred to in the literature [48] as a surface spin wave mode, since the spin wave is mostly localized near the surface due to attenuation. Increasing α de-localizes the spin-wave near the surface, compare Figs. 5 and 6 for imaginary k values.

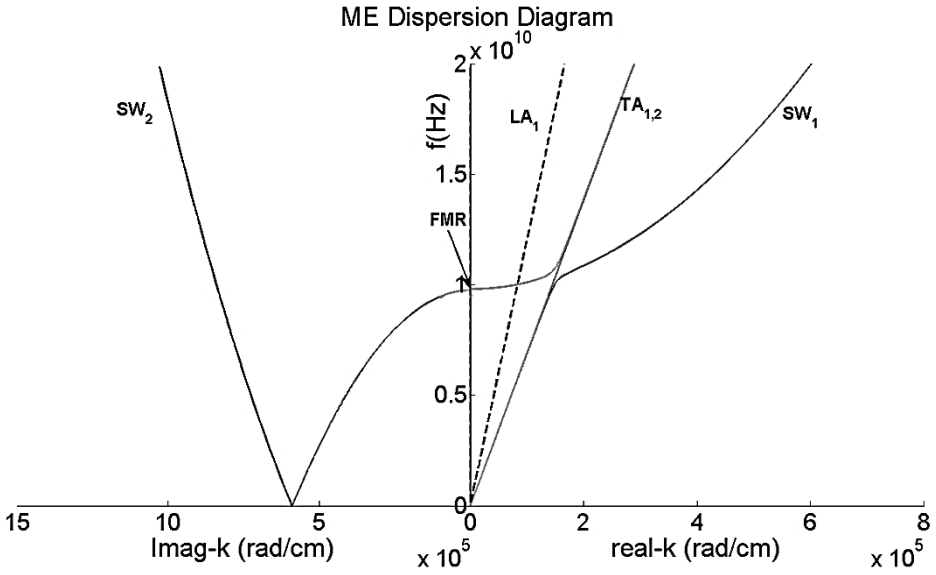

Fig. 5 Plot of dispersion relation between frequency and Re and Im(k) for α = 1.

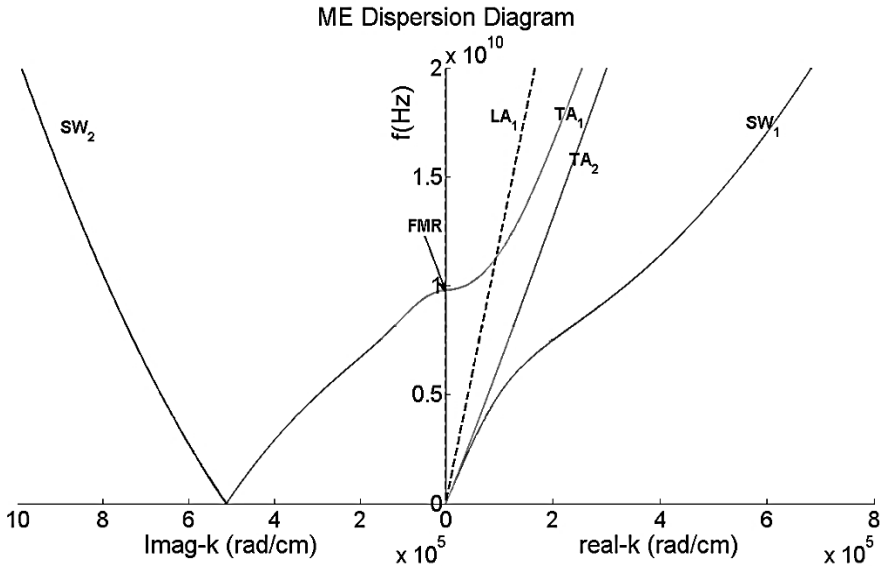

Fig. 6 Plot of dispersion relation between frequency and Re and Im(k) for α = 10.

The splitting of the cross coupling between one of the TA and SW_1 branches is proportional to the product of α , d_5 and C_{44}. For example, we varied the value of α between 0.3 and 10.0 (CGS units) and calculations of the dispersion indicate: (1) The spitting increased proportionally with α . (2) For low values of k the modes are an admixture of spin waves and acoustic transverse modes. The longitudinal acoustic mode is unaffected by the magnetic modes (see Figs. 5-6). However, in some special experimental conditions the longitudinal mode can be made to interact with the magnetic modes. Interaction between spin waves and longitudinal acoustic waves may be actuated by applying H in the film plane. For this field configuration the normal modes of magnetic FMR precession are m_x and m_z . Whereas m_x may couple to U_x , m_z may couple to U_z via the ME coupling. Thus, all of the acoustic branches would couple to the spin wave branch. We anticipate that the coupling between branches would not be uniform, since usually $C_{33} \neq C_{44}$ and $d_5 \neq d_3$[39]. However, invoking an anisotropic α would allow for interaction between volume spin wave modes and longitudinal acoustic branches or modes.

Clearly, the spin wave dispersion no longer obeys the k^2 law for frequencies near FMR, especially for high values of α (see Fig. 6). For example, in a standard standing spin wave (SWR) resonance experiment [49] the resonant field positions usually obey the n^2 law, n is the SW order number. It is noted that this branch admixes with the TA branch such that it's dispersion increases faster than k^2 as it transitions to a TA mode. In fact, at high frequencies and high α values the two TA modes are no longer degenerate. Excitations of standing spin wave modes may be possible in ME films of ~1 micron in thickness and exposing the film to an h field excitation. Standing TA modes may be excited in a similar manner by exposing the ME sample to e field excitations. However, these dispersions imply that the nature of the fields within the ME sample may transition from one type of field excitation to another form of field excitation depending on the frequency of operation.

In the calculation of the dispersion relationships as shown in Figs. 5-6 H_0 was fixed at 3500 Oe and, therefore, H = 4500 Oe. It is possible in ME hexaferrites to choose a sample such that $4\pi M \sim H_{ss}$ so that zero field FMR may be observed. The advantage of this situation or experimental condition is that internal static and dynamic fields induced by the ME effect begin to compete with fields that allow for ordinary zero field FMR. For example, for α =3.2 the dispersions are shown in Fig. 7. FMR occurs for H_0 = 100 Oe or 280 MHz. This plot is very reminiscent of Fig. 6 except that FMR is at much lower fields or frequencies. Here again the two TA modes are no longer degenerate, and the same observations about Fig. 6 also applies here. With the application of a static electric field of E ~ 20,000 v/m, we see a dramatic change in the dispersions. For example, a voltage of 20 mv across the film thickness would be sufficient to generate a static magnetic field of 20 Oe. Basically, SW_1 branch has flip-flopped with the SW_2 branch, see Figs. 7-8. Also, FMR frequency was lowered to 224 MHz. In addition to the ordinary FMR mode at $\frac{\omega}{\gamma} = H_0$ (280 MHz), there is an extraneous FMR mode at approximately $\frac{\omega}{\gamma} \approx H_0 - M(\alpha d_4)^2 C_{44}$. It is predicted that for the parameters chosen above, the FMR frequency of the extraneous mode occurs at approximately ~ 40 MHz which corresponds to the lower resonance at k = 0. Thus, it appears that there are two FMR modes at k = 0. Ordinarily, there is only one uniform precession mode at k = 0. Also, the character of the wave (either spin wave or acoustic) changes upon application of a static electric field. Thus, the effect of the α coupling is quite pronounced and it has the greatest impact on dispersions, at low frequencies (~MHz ranges). We believe that these type of effects are important to potential new applications and future ME experiments.

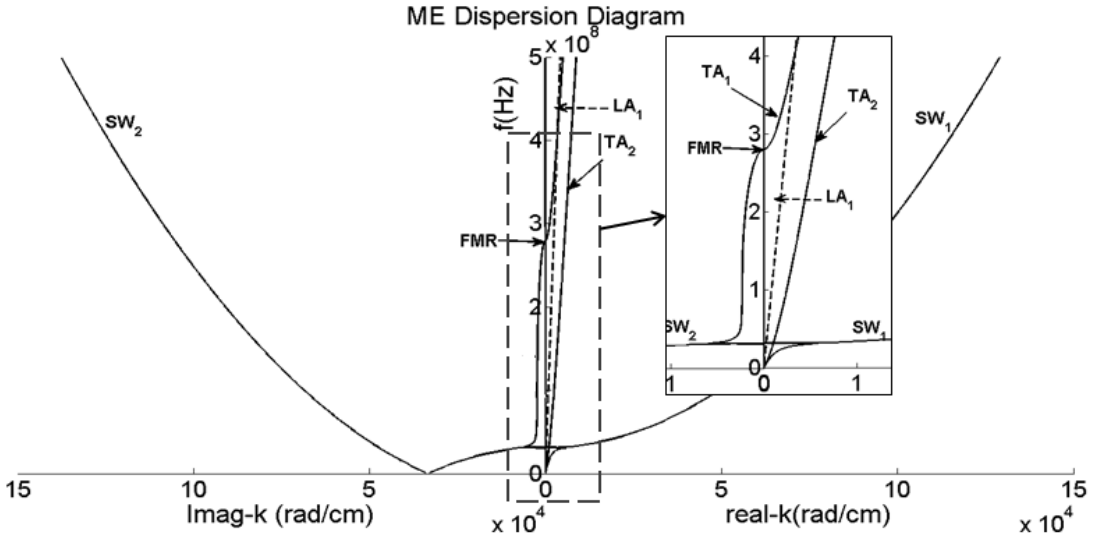

Fig. 7 Frequency versus propagation constant, k, for α=3.2, H_0=100, and E = 0.

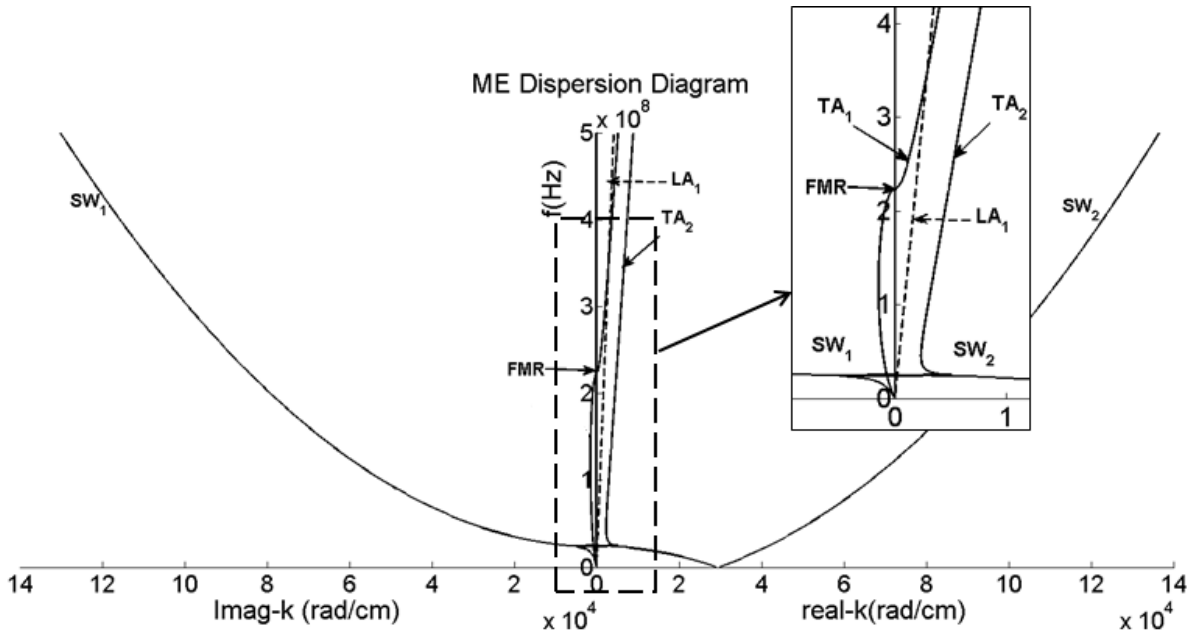

Fig. 8 Frequency versus propagation constant, k, for α=3.2, H_0=80, and E = 20,000v/m (~ 20 Oe).

As in Figs. 5-6 the TA_1 acoustic mode transitions into a surface spin wave mode, see Figs. 7-8. The electromagnetic (em) branch has been omitted so far in the dispersion relation above. The inclusion of the em branch would modify only the SW branches, since k ~ 3rad/cm at 10 GHz, for example. The k values of the acoustic branches extend well beyond 3 rad/cm at the same frequency so that no coupling between the em branch and acoustic branches is expected. However, at low frequencies, where zero field FMR may be excited, the em branch may couple to all branches. The dynamic magnetic field, $\vec{h}$, in the magnetic equation of motion is coupled to the electric field, $\vec{e}$, in Maxwell's equations giving rise to the em branch. By uncoupling Maxwell's equations $\vec{h}$ may be expressed in terms of $\vec{m}$. As such, Maxwell's equations are directly coupled into the magnetic equations of motion. A simpler way (see appendix) to introduce electromagnetic modes or branches in eq. (24) is to make the "transformation" in the dispersion relation of eq. (24) that

$$H_0 \Rightarrow H_0 + \frac{4\pi M}{1-\dfrac{k^2}{\omega^2 \varepsilon}} \ .$$

V Conclusions and Discussions

There have been many reports about ME effects on static field changes of electrical polarization and magnetization upon the application of static fields. We have introduced a formalism by which static and/or dynamic internal fields can be accounted for upon application of static or dynamic electric or magnetic fields. The static field measurements [45] seem to confirm the view proposed

by Landau-lifshitz that the spin spiral configuration can be described by a simple uniaxial magnetic anisotropy energy term only. Experimentally [45], the inclusion of the uniaxial magnetic anisotropy field in the FMR condition is consistent with a g value of ~ 2 for ME hexaferrites. Our calculations predict FMR resonance shifts in the order of 5-20 Oe with the application of a static electric field or DC voltage in the order of 1 volt or less in films. This prediction should be compared with measured shifts of 0.2 Oe in Ref. [50] using impure bulk lithium ferrites at very high DC voltages (~ 500 volts). Furthermore, it is predicted at low frequencies (~MHz ranges), near zero magnetic field FMR frequencies, there is an extra uniform precession FMR mode besides the ordinary FMR mode which can only be accounted by magneto-electric α coupling fields. Whereas the FMR frequency shifts in the ordinary FMR mode due to the α coupling scale as α, the shifts in the new discovered FMR mode scale as α^2 . For example, for k = 0 there are two FMR resonant modes: one FMR mode is characterized as an ordinary mode resonating at 280 MHz and the extraneous mode resonates at 40 MHz.

Also, magneto-elastic dispersions were calculated and it is predicted that the effect of the α coupling are the following: 1. The strength of admixture of modes and splitting in energy between spin waves and transverse acoustic waves is proportional to α. 2. The degeneracy of the two transverse acoustic wave modes is lifted even for relatively low values of α. Interestingly, at low frequencies near zero field FMR frequencies the surface spin wave mode branch flip-flops with the volume spin wave branch whereby one branch assumes real values of the propagation constant and the other purely imaginary upon the application of a static electric field.

Magneto-elastic excitations in ME hexaferrites may be generated or established with the application of localized dynamic e and h fields setting up standing modes in finite dimensionalities of samples. The effect of α on the dispersion is quite dramatic at low as well as at high frequencies even for values of α not exceedingly high (in MKS units $\alpha \sim 10^{-8}$). We believe that the impact of ME hexaferrites to modern day technologies and science will be felt in the near future even though the upper limit in α values has not been reached yet.

Appendix

Re-writing the equations of motion with $\vec{h}$ included one obtains

$$j\frac{\omega}{\gamma}m_x = m_y(H_0 + \frac{2A}{M^2}k^2) - M\alpha p_y - Mh_y \text{ , and}$$

$$j\frac{\omega}{\gamma}m_y = -m_x(H_0 + \frac{2A}{M^2}k^2) + M\alpha p_x + Mh_x .$$

The equations expressed as above lend themselves readily to the calculation or determination of magnetic susceptibilities in a tensor form [χ_m]. After uncoupling Maxwell's equations and assuming propagation in the z-direction the relationships between $\vec{h}$ and $\vec{m}$ become [35]

$$h_x = \frac{4\pi m_x}{\frac{k^2}{\omega^2 \varepsilon} - 1} \quad ,$$

$$h_y = \frac{4\pi m_y}{\frac{k^2}{\omega^2 \varepsilon} - 1} \quad \text{, and}$$

$$h_z = -4\pi m_z \quad .$$

In a linear excitation $m_z \sim 0$. By substituting above relationships into the equations of motion for the normal modes one obtains

$$j\frac{\omega}{\gamma} m_x = m_y[(H_0 + \frac{4\pi M}{1 - \frac{k^2}{\omega^2 \varepsilon}}) + \frac{2A}{M^2} k^2] - M\alpha p_y \quad \text{, and}$$

$$j\frac{\omega}{\gamma} m_y = -m_x[(H_0 + \frac{4\pi M}{1 - \frac{k^2}{\omega^2 \varepsilon}}) + \frac{2A}{M^2} k^2] + M\alpha p_x \, .$$

This proves that the above ad-hoc transformation may be substituted in the dispersion relation, eq. (24).

I want to thank Saba Zare for her help in putting this manuscript together in all phases. Also, we want to thank the support of the NSF (grant # 1002543) and ARO (grant # W911NF-14-1-0630).

References

1. T. Kimura, *Magnetoelectric hexaferrites.* Annu. Rev. Condens. Matter Phys., 2012. 3(1): p. 93-110.
2. Tokunaga Y, Kaneko Y, Okuyama D, Ishiwata S, Arima T, et al. 2010. Phys. Rev. Lett. 105:257201.
3. Y. Tokunaga, Y. Kaneko, D. Okuyama, S. Ishiwata, T. Arima, S. Wakimoto, K. KakuraiY. Taguchi, and Y. Tokura, Phys. Rev. Lett. 105(25), 25720(2010).
4. S. Ishiwata, T. Taguchi, H. Murakawa, Y. Onose, and Y. Tokura, Science 319, 1643(2008).
5. Y. Hiraoka, H. Nakamura, M. Soda, Y. Wakabayashi, and T. Kimura, J. Appl. Phys. 110, 033920(2011).
6. K. Tamiguchi, N. Abe, S. Ohtani, H. Umetsu, and T.H. Arima, Appl. Phys. Express 1, 1301(2008).
7. M. Soda, T. Ishikura, H. Nakamura, Y. Wakabayashi, and T. Kimura, Phys. Rev. Lett. 106, 087201(2011).
8. T. Kato, H. Mikami and S. Noguchi, J. Appl. Phys. 108, 033903(2010).
9. S. Ishiwata, Y. Taguchi, H. Murakawa, Y. Onose and Y. Tokura, Phys. Rev. B81, 174418(2010).
10. L. Wang, D. Wang, Q. Cao, Y. Zheng, H. Xuan, J. Gao, and Y. Du, Nature Scientific reports, 2012.

11. M. Mohebbi, and C. Vittoria, *J. Appl. Phys*. **113,** 17C703 (2013).
12. B. B. Van Aken, T. T. Palstra, A. Filipetti, and N. A. Spaldin, Nature Materials 3(3), 164(2004).
13. R. E. Newnham, J. Kramer, W. Schulze, and L. Cross, J. Appl. Phys. 49, 6088(1978).
14. V. Y. Pomjakushin, M. Kenzelmann, A. Donni, A. Harris, L. Keller, T. Nakajima, and H. Kitazava, J. Appl. Phys. 11(4), 043019(2009).
15. M. Kenzelmann, A. Harris, S. Jonas, C. Broholm, J. Schefer, S. Kim, C. Zhang, S.-W. Cheong, O. Vajk, and J. Lynn, Phys. Rev. Lett. 95(8),087206(2005).
16. J. Wang, J. Neaton, H. Zheng, V. Nagarajan, S. Ogale, B. Liu, D. Viehland, V. Vaithyanathan, D. Schlom, and U. Waghmare, Science, 2003. 299(5613): p. 1719-1722.
17. T. Goto, T. Kimura, G. Lawes, A. Ramirez, and Y. Tokura, Phys. Rev. Lett. 92(25), 257201(2004).
18. G. Srinivasan, Annual Review of Materials Research 40, 153-178(2010).
19. Khabat Ebnabbasi, and Carmine Vittoria, Phys. Rev. B86, 024430(2012).
20. L. D. Landau and E.M. Lifshitz, Electrodynamics of Continuous Media, pp.178 Pergamon Press, Oxford Press, Oxford (1984).
21. Dzyaloshinskii I. *J. Phys. Chem. Solids* **4** 241–55 (1958).
22. Moriya M. *Phys. Rev.* **120** 91–98 (1960).
23. W.P.Wolf, Phys. Rev. 108, 1152(1957).
24. D.N. Astrov, *Soviet Physics JETP* **11**, 708(1960).
25. V.J. Folen, G.T. Rado, and E.W. Stalder, *Phys. Rev. Lett.* **607** (1961).
26. H. Katsura, N. Nagaosa, and A.V. Balatsky, Phys. Rev. Lett. 95, 057205(2005).
27. T. Kimura, Annu. Rev. Mater. Res., 2007. 37: p. 387-413.
28. M. Mostovoy, Phys. Rev. Lett. 96(6), 067601(2006).
29. M. Feng, B. Shao,J. Wu, and X. Zuo, J. Appl. Phys. 113, 17D909(2013).
30. Sergienko IA, Dagotto E. *Phys. Rev. B* **73** 094434 (2006).
31. M. Fiebig, Journal of Physics D: Applied Physics 38(8), R123(2005).
32. Carmine Vittoria, Somu Sivasubramanian and Allan Widom, Phys. Rev. B89, 134413(2014).
33. E.P. Wohlfarth, *Handbook of Magnetic Materials: A Handbook on the Properties of Magnetically Ordered Substances*. Vol. 2. 1980: Access Online via Elsevier.
34. Marjan Mohebbi, Ph.D. Thesis, Magnetoelectric effects in M-type hexaferrites,Northeastern University(2014).
35. J. Smit and H. Wijn, *Ferrites Philips Technical Library.* Eindhoven, The Netherlands, 1959: p. 157.
36. G. Albanese, A. Deriu, and S. Rinaldi, Journal of Physics C: Solid State Physics 9(7), 1313(1976)
37. Carmine Vittoria, Magnetics, Dielectrics and Wave Propagation with MAT/ LAB Codes, CRC Press, New York (2010).
38. Landolt-Bornstein, Numerical Data and Functional Relationships in Science and Technology,Vol. 4,Springer-Verlag, Berlin(1970).
39. B.A. Auld, *Acoustic fields and waves in solids*. Vol. 1. 1973: Wiley New York.
40. W. Mason, *Derivation of magnetostriction and anisotropic energies for hexagonal, tetragonal, and orthorhombic crystals.* Physical Review, 1954. 96(2): p. 302.
41. S. Chikazumi, Physics of Magnetism, John Wiley and sons, Inc., New York (1964).
42. E. Fatuzzo and W. J. Merz, Ferroelectricity, John Wiley and Sons, Inc., New York(1967).
43. J. Smit and H. G.Beljers, Phillips Res. Rep. 10, 113(1955).
44. F. J. Rachford, P. Lubitz and C. Vittoria, J. Appl. Phys. 53, 8949(1982).
45. K. Ebnabbasi, Ph.D. Thesis, Northeastern University(2013); H. Izadkhah,S. Zare, S. Sivasubramanian, and C. Vittoria, Appl. Phys. Lett. 106, 142905(2015).
46. L. D. Landau and E. M. Lifshitz, Mechanics, vol. 1, Pergamon Press, New York(1976).
47. C. Kittel, Phys. Rev. 110, 836(1958).
48. W. S. Ament and G. T. Rado, Phys. Rev. 97, 1558(1955).
49. G. C. Bailey and C. Vittoria, Phys. Rev. B8, 3247(1973).

50. G. T. Rado, C. Vittoria, J. Ferrari and J. P. Remeika, Phys. Rev. Lett. 41, 1253(1978).